JOURNAL OF COMPUTATIONAL PHYSICS 46, 454–461 (1982)

Space-Charge Effects in High-Density Plasmas

R. MORROW

Division of Applied Physics, CSIRO,
Sydney, New South Wales 2070, Australia

Received October 14, 1981

The electron and ion continuity equations and Poisson's equation are solved for the motion of a pulse of plasma of peak density up to 10^{13} cm^{-3}, in nitrogen at 12 kPa, with an initially uniform electric field of −5.58 kV/cm. Slight movement of the electrons causes the electric field to be reduced to almost zero throughout the plasma and enhanced outside the plasma. The net charge has a positive peak near the cathode and a negative peak near the anode and varies smoothly from one to the other throughout the plasma. It is possible to obtain results at these higher densities by (i) the use of the flux-corrected transport algorithm of Boris and Book, "Phoenical LPE Shasta," together with Zalesak's flux limiting algorithm, and (ii) the limiting of the time step to avoid a numerical instability. The numerical instability at these high densities is found to be an oscillation in the calculated electric current due to too great a change in the electric field in one time step. With a suitable limitation in the time step, calculations can be performed at much higher plasma densities.

1. INTRODUCTION

In a recent paper [1] we presented the results of the effects of space-charge fields on the motion of electrons and ions for peak densities up to 5×10^{11} cm^{-3}. The method used was the two-step Lax–Wendroff method and, due to numerical dispersion and a numerical instability, it was not possible to perform calculations for higher density plasmas at that time.

In this paper it is shown how calculations can be performed at much higher densities, 10^{13} cm^{-3} in this case, using a flux corrected trnasport (FCT) algorithm due to Boris and Book [2], provided the time step is limited to avoid a space-charge-driven numerical oscillation. A detailed comparison of the FCT method with other available methods is given elsewhere [3]. The FCT method introduces less numerical dispersion and diffusion than the other methods examined. Furthermore, it is more stable for the sharp discontinuities in the physical parameters encountered in high density plasmas. The FCT method also allows a small amount of diffusion to be included in a more convenient way than has been presented previously. Nevertheless, the FCT method does not take a significantly longer computing time than the two-step Lax–Wendroff method. The particular FCT algorithm used is the "Phoenical LPE Shasta" method with the modified flux correction algorithm of Zalesak [4].

0021-9991/82/060454–08$02.00/0

In general, for the explicit solution of hyperbolic equations, the time step Δt is limited by the Courant–Friedrichs–Lewy condition which requires that $\Delta t < \Delta x/W$, where Δx is the grid space and W the velocity [5]. For the FCT method this condition becomes $\Delta t < \Delta x/2W$; however, for very high densities the change in electric field ΔE in one time step due to space charge movements is comparable to E_0, the initial field, and numerical oscillations occur. These oscillations are best displayed by calculating the external-circuit electric current which illustrates the back–and–forth motion of the charges. This problem is overcome by limiting the time step and, in principle, calculations can be performed without an upper limit on the density.

2. Problem To Be Solved

2.1. *Equations*

The equations to be solved simultaneously are the drift-dominated continuity equations for electrons and ions in one-dimensional conservative form. Source terms are neglected, but slight electron diffusion is included. The equations are

$$\frac{\partial N_e}{\partial t} = -\frac{\partial (N_e W_e)}{\partial x} + \frac{\partial}{\partial x}\left(D \frac{\partial N_e}{\partial x}\right) \tag{1}$$

and

$$\frac{\partial N_p}{\partial t} = -\frac{\partial (N_p W_p)}{\partial x} \tag{2}$$

where N_p and N_e are ion and electron densities, respectively, and W_p and W_e are electric-field-dependent ion and electron velocities, respectively. The effect on the electric field of space charge, due to ion and electron concentrations, is obtained by solving Poisson's equations

$$\nabla E = -\zeta/\varepsilon_0 \tag{3}$$

where ε_0 is the permitivity of free space, ζ the charge density given by

$$\zeta = e(N_p - N_e) \tag{4}$$

and e the electronic charge.

To account correctly for the space-charge field due to a finite charge distribution, it is necessary to solve Poisson's equation in three dimensions, as discussed by Davies *et al.* [6]. We use the method of Davies and Evans [7] to account for these effects and solve for a cylinder of charge, which gives the field at a point P due to a charge distribution $\zeta(x)$ by a simple geometric integration. Five image charge distributions beyond each electrode are also included.

We calculate the electric current in the external circuit due to the motion of electrons and ions between the electrodes using an equation developed by Sato [8],

$$I = \frac{\pi r^2 e}{V_A} \int_0^d (N_p |W_p| + N_e |W_e|) E_0 d_x \tag{5}$$

where I is the external-circuit current in amperes, V_A is the applied voltage, E_0 the initial field in the absence of space charges, r the discharge radius, e the electron charge, and d the electrode separation.

2.2. *Initial Conditions*

The physical parameters have been discussed in detail by Morrow and Lowke [1]. Briefly, the plasma moves between parallel plates 3 cm apart in an initially uniform electric field of −5.58 kV/cm. This space is represented by a grid of 201 points, hence $\Delta x = 0.015$ cm. The initial Gaussian electron and ion distributions are identical and overlap to give a neutral plasma with no field distortion. The distributions are cylindrical with a diameter of 0.5 cm, over which the densities are constant, while in the axial direction the density varies as

$$N_e = N_p = N_0 \exp\{-[(x - 1.5)/0.25]^2\} \quad \text{cm}^{-3} \tag{6}$$

The time step used is variable in this case, as discussed below.

3. Numerical Methods

Since Boris and Book present many alternative FCT algorithms, some detail of the particular algorithm used will be presented. This also allows an explanation of the method of introducing a realistically small amount of diffusion. The Phoenical LPE Shasta method involves the following steps:

1. Compute a transported and diffused intermediate solution N_i^{*j+1} using

$$\begin{aligned} N_i^{*j+1} = N_i^j &- \tfrac{1}{2}[\varepsilon_{i+1/2}(N_{i+1}^j + N_i^j) - \varepsilon_{i-1/2}(N_i^j + N_{i-1}^j)] \\ &+ [\nu_{i+1/2}(N_{i+1}^j - N_i^j) - \nu_{i-1/2}(N_i^j - N_{i-1}^j)] \end{aligned} \tag{7}$$

where N is the number density, j refers to the time step, and i refers to the grid position, $\varepsilon_{i+1/2} = W_{i+1/2} \cdot \Delta t/\Delta_x$ and $W_{i+1/2}$ is the drift velocity half way between grid points i and $i+1$, calculated in this case by simple averaging. For the Phoenical LPE version of the Shasta algorithm the diffusion coefficient is

$$\nu_{i+1/2} = \tfrac{1}{6} + \tfrac{1}{3}\varepsilon_{i+1/2}^2.$$

2. Compute the raw antidiffusive fluxes, which in the case of the Phoenical version are

$$\phi_{i+1/2} = \mu_{i+1/2}\,[N_{i+1}^{*j+1} - N_i^{*j+1} + (-N_{i+2}^{j} + 3N_{i+1}^{j} - 3N_i^{j} + N_{i-1}^{j})/6] \tag{8}$$

where $\mu_{i+1/2} = (1 - \varepsilon_{i+1/2}^2)/6$, the antidiffusion coefficient.

3. Compute corrected antidiffusive fluxes $\bar{\phi}$ using

$$\bar{\phi}_{i+1/2} = S \max\{0, \min[S(N_{i+2}^{*j+1} - N_{i+2}^{*j+1}), |\phi_{i+1/2}|, S(N_i^{*j+1} - N_{i-1}^{*j+1})]\} \tag{9}$$

where $|S| = 1$ and $S = \text{sign}(N_{i+1}^{*j+1} - N_i^{*j+1})$.

4. Perform antidiffusion using

$$N_i^{j+1} = N_i^{*j+1} - \bar{\phi}_{i+1/2} + \bar{\phi}_{i-1/2} \tag{10}$$

Thus N_i^{j+1} is the required solution at $t + \Delta t$, without any significant numerical diffusion or dispersion. Simultaneous calculations of this type are carried out for the ion and electron densities.

Step 3, however, was replaced by the new algorithm for flux limiting developed by Zalesak [4] as outlined in Section 4 of this paper. The method of avoiding "clipping" by predicting maxima and minima between grid points for use in flux limiting, outlined in Section V of Zalesak's paper, was also applied. The advantages in using this approach have been examined in detail by Morrow [3].

At the upstream electrode (i.e., generally the cathode for electrons and anode for ions), we impose boundary conditions of $N_e = 0$ and $N_p = 0$. At the downstream electrode, we use upwind differencing to evaluate the drift terms in Eqs. (1) and (2) [9].

As outlined by Boris and Book [2] the introduction of a small amount of diffusion is quite simple with this method. If $\delta_{i+1/2}$ is the required diffusion coefficient at $i + \frac{1}{2}$, then this is expressed in dimensionless form and subtracted from the antidiffusion coefficient, $\mu_{i+1/2}$, such that the new antidiffusion coefficient $\mu'_{i+1/2}$ is given by

$$\mu'_{i+1/2} = \mu_{i+1/2} - \delta_{i+1/2}\,\Delta t/(\Delta x)^2 \qquad \text{provided} \quad \mu'_{i+1/2} \geqslant 0. \tag{11}$$

The current in the external-circuit was calculated at each time step by numerically integrating Eq. (5) using the trapezoidal rule [10].

The time step was calculated using

$$\Delta t = K\,\Delta x / W_e^{\max} \tag{12}$$

where $W_e^{\max}$ is the maximum value of the electron velocity and $K \leqslant 0.25$. Before the onset of numerical instability, $K = 0.25$ is used, so that the FCT rule $\Delta t < \Delta x/2w$ is obeyed. As shown below, K must be considerably reduced as the density is increased.

4. Results

4.1. *Plasma Motion*

Results are presented in Fig. 1 for a plasma of peak density, $N_0 = 10^{13}$ cm^{-3}, for the first 14 ns. The number of computational steps was 800 and the average time step was 0.018 ns. The time step was determined using Eq. (12), with $K = 0.05$.

The motion of the electrons relative to the ions is very slight as shown in Fig. 1a,

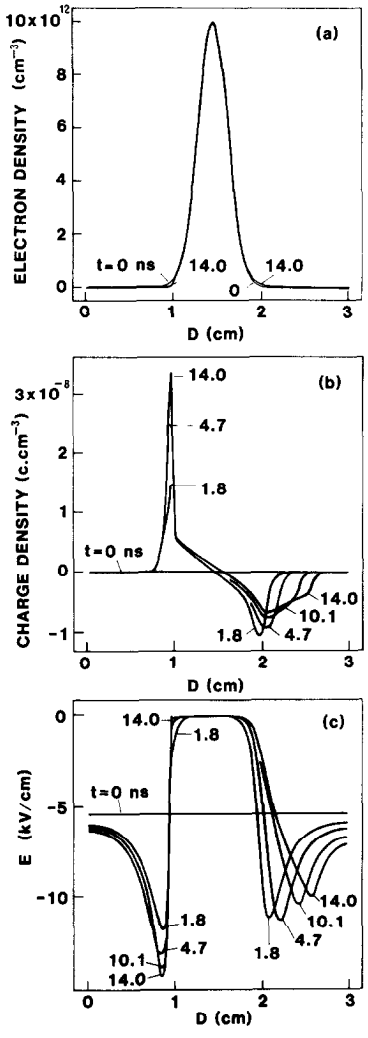

FIG. 1. Calculations of plasma motion and space-charge electric fields using FCT method with $E_0 = -5.58$ kV/cm, $N_0 = 10^{13}$ cm^{-3}, and $K = 0.05$. Calculations are for 800 steps and a time of 14-ns. Curves are shown for $t = 1.8$, 4.7, 10.1, and 14 ns. (a) Electron and ion density distribution, (b) charge distribution, (c) total electric field.

while the ions do not move significantly. The electron distribution shows similar characteristics to those discussed for lower density plasmas by Morrow and Lowke [1]. The trailing edge of the electron distribution becomes quite steep, while the escaping electrons have a flat distribution.

This motion is hardly perceptible in Fig. 1a but becomes clearer when the charge is calculated, as shown in Fig. 1b. Near $D = 1$ cm there is a large positive peak in the charge density, which is responsible for the large field outside the plasma, and low field inside the plasma (see [1]). The positive peal becomes larger with time, as electrons are driven into the plasma, and the right-hand edge of the positive peak becomes very steep, corresponding to the steep trailing edge of the electron distribution. Near $D = 2$ cm, there is a similar peak of negative charge, which becomes flatter as electrons begin to escape [1]. Between the positive and negative peaks there is a steady change throughout the plasma from positive charge near the cathode to negative near the anode, with the charge being zero only near $D = 1.5$ cm. This internal charge distribution is necessary to give the essentially zero field inside the plasma shown in Fig. 1c. The positive peak in the charge density reduces the field inside the plasma to zero; however, the field would then rise again if more positive charge was not distributed closer to the center of the plasma. As shown in Fig. 1c, $\partial E/\partial x \approx 0$ and $\partial E/\partial x \neq -\zeta/\varepsilon$, because the finite dimensions of the plasma require the field to be calculated using Poisson's equation (Eq. (3)) in three dimensions [11].

The results for the electric field calculation, shown in Fig. 1c. are very similar to those presented for a peak density of 5×10^{11} cm^{-3} by Morrow and Lowke [1]. The field within the plasma, however, is more uniform and approaches zero more closely near $D = 1.5$ cm, where the field is $E \approx -8$ V/cm.

4.2 *Numerical Instability*

The time step was determined using Eq. (12), where the Courant–Friedrichs–Lewy condition requires $K < 1$ and the FCT algorithm requires that $K < 0.5$. These restrictions, however, relate to the transport algorithm, and take no account of the change in electric field caused by the movement of charge. Thus, at high density, the transport algorithm will allow in one time step a movement of charge sufficient to reverse the driving field, i.e., $\Delta E > E_0$. The electron motion is then reversed, and a step-by-step numerical oscillation develops, giving an oscillating electric current, shown in Fig. 2a for the same conditions as Fig. 1, except that $K = 0.1$. This result shows the extraordinary stability of the FCT method, because, as the numerical oscillation damps out, the solution converges to that shown in Fig. 1. A reduction in the value of K to $K = 0.05$ gives the result shown in Fig. 2b, which is the current corresponding to the results of Fig. 1, and which shows no sign of instability.

For a peak density of 5×10^{12} cm^{-3}, the instability occurs for $K = 0.25$, but the results are stable for $K = 0.1$. Thus, to a first approximation, the limit on Δt is inversely proportional to N_0. Basically, however, it is the change in the electric field in one time step that must be limited to some fraction of, say, the initial field and this can be implemented automatically in the computer program.

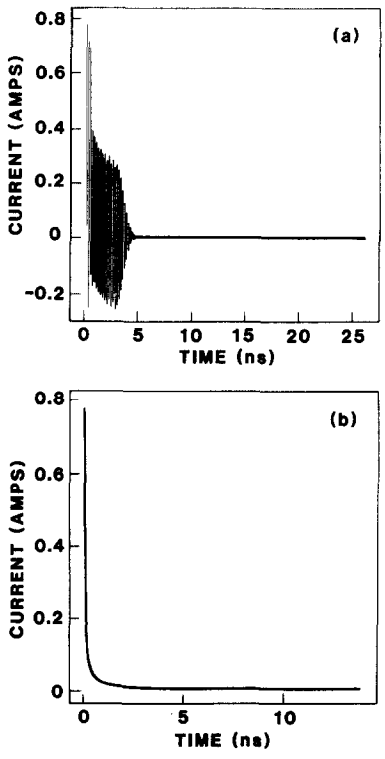

FIG. 2. Calculations of the external-circuit current versus time due to ion and electron motion using Sato's (Eq. 5)) for $E_0 = -5.58$ kV/cm and $N_0 = 10^{13}$ cm^{-3}. (a) Current calculated with $K = 0.1$, (b) current calculated with $K = 0.05$, corresponding to the results of Fig. 1.

4.3 *Computer Time*

For an identical problem, the central processor time used for the two-step Lax–Wendroff method was 9.9 s while for the FCT method the time used was 12.3 s. Thus the penalty for the extra complexity and stability is not very great.

5. CONCLUSIONS

A plasma pulse of volume $\sim(0.5)^3$ cm^3 and density $\sim 10^{13}$ cm^{-3} is very stable and the application of an electric field $\sim$6 kV/cm causes an almost imperceptible movement of the electron distribution. The electric field, however, is almost entirely excluded from the body of the plasma. The charge distribution shows that electrons move relative to the ions throughout the plasma, giving a steady gradient in charge from positive to negative in the plasma. Thus, charge neutrality does not hold for a finite plasma in a electrc field. The movement of charges that produces the result

$\partial E/\partial x \approx 0$ in the plasma does not require the charge to be zero, because, for a finite plasma, Poisson's equation must be solved in three dimensions.

The numerical instability at high densities results from too large a change in the electric field within one time step causing a numerical charge oscillation. Recognition of this limitation on the time step allows results to be obtained at comparatively high densities.

These results show the great stability of the FCT method with the most extreme nonuniformities in charge density and electric field. The ability of the algorithm to converge onto the correct solution when thrown completely off course by the use of too large a time step gives considerable support for and confidence in the method.

REFERENCES

1. R. MORROW AND J. J. LOWKE, *J. Phys. D.* **14** (1981), 2027.
2. J. P. BORIS AND D. L. BOOK, *Methods Comput. Phys.* **16** (1976).
3. R. MORROW, *J. Comput. Phys.* **43** (1983), 1.
4. S. T. ZALESAK, *J. Comput. Phys.* **31** (1979), 335.
5. D. POTTER, "Computational Physics," Wiley, New York, 1977.
6. A. J. DAVIES, C. S. DAVIES, AND C. J. EVANS, *Proc. Inst. Elec. Eng.* **118** (1971), 816.
7. A. J. DAVIES AND C. J. EVANS,"Theory of Ionization Growth in Gases under Pulsed and Static Fields," Report to CERN European Organization for Nuclear Research, Geneva, 1973.
8. N. SATO, *J. Phys. D.* **13**, (1980) *L*3.
9. P. J. ROACHE, "Computational Fluid Dynamics," Hermosa, Albuquerque, N. M., 1972.
10. M. ABRAMOWITZ AND I. A. STEGUN, "Handbook of Mathematical Functions," Dover, New York, 1965.
11. A. J. DAVIES AND C. J. EVANS, *Proc. Inst. Elec. Engrg.* **114**, (1967), 1547.